From Ionic Clusters Dynamics to Network Constraints in Ionic Polymer Solutions

Sidath Wijesinghe,[1,3] Chathurika Kosgallana,[1*] Manjula Senanayake,[1,&] Supun S. Mohottalalage,[1,#] Piotr Zolnierczuk,[4] Laura Stingaciu,[4] Gary S. Grest[5*] and Dvora Perahia[1,2*]

[1] Department of Chemistry, Clemson University, Clemson, South Carolina 29634, USA
[2] Department of Physics, Clemson University, Clemson, South Carolina 29631, USA
[3]Department of Chemistry, Appalachian State University, Boone, North Carolina 26808, USA
[4]Neutron Scattering Division, Oak Ridge National Laboratory, Oak Ridge, Tennessee 37831, USA
[5]Sandia National Laboratories, Albuquerque, New Mexico 87175, USA

Physical networks formed by ionizable polymers with ionic clusters as crosslinks are controlled by coupled dynamics that transcend from ionic clusters through chain motion to macroscopic response. Here the coupled dynamics, across length scales, from the ionic clusters to the networks in toluene swollen polystyrene sulfonate networks, were directly correlated, as the electrostatic environment of the physical crosslinks was altered. The multi-scale insight is attained by coupling neutron spin echo measurements with molecular dynamics simulations, carried out to times typical of relaxation of polymers in solutions. The experimental dynamic structure factor is in outstanding agreement with the one calculated from computer simulations as the networks are perturbed by elevating the temperature and changing the electrostatic environment. In toluene, the long-lived clusters remain stable over hundreds of ns across a broad temperature range, while the polymer network remains dynamic. Though the size of the clusters changes as the dielectric constant of the solvent is modified through addition of ethanol, they remain stable but morph, enhancing the polymer chain dynamics.

I. Introduction

Ionizable polymers form networks through physical crosslinks of clustered ionizable groups. The heterogeneity of the structure and response of these complex networks enables their many applications, ranging from biotechnology to clean energy generation and storage [1-4]. In contrast to chemically crosslinked networks, the clusters constitute a dynamic bridge whose properties affect the network behavior in melts and in solutions [5-7]. Determining coupled dynamics across distinctive length scales remains a challenging open question, fundamental to these complex networks, and critical to the design of ionizable polymers assemblies for targeted applications. Combining neutron spin echo (NSE) measurements with groundbreaking atomistic-level molecular dynamics (MD) simulations, a direct correlation between dynamics of intra-cluster events to network motion was attained. Reaching time scales of polymer chains dynamics in solutions was enabled by exascale computing and is a key to bridging between length scales. NSE probes mesoscopic length scales (0.5-40 nm) on a time scale of up to ~150 ns here and MD simulations access intra-cluster dynamics in correlation with that of the mesoscopic response of the networks. With direct correlations between results attained by these two techniques, we find that small variations in intra-cluster correlations induced by changing solvent polarity, is sufficient to impact the mesoscopic network dynamics. This provides a direct molecular insight into a long-standing open question of the origin of macroscopic constraints in physical networks with dynamic crosslinks.

The dynamic processes across length scales of networks formed by a model polymer, sulfonated polystyrene (SPS) in toluene, a good solvent for the backbone and poor for the polar groups, are probed as the systems are perturbed by increasing the temperature and adding a polar solvent. Pioneering studies of Weiss and coworkers demonstrated the confining effects of ionic clusters

on the rheology of SPS solutions [8-13]. Early NSE studies of SPS [14,15] further affirmed that the ionic clusters confine segmental dynamics in solutions. Our recent NSE-MD study of SPS in toluene [7] have shown that while the network dynamics is constraint by the clusters, the highly solvated individual polymer chains remain dynamic.

The realization that clusters affect the structure and dynamics of these has driven several studies where their electrostatic environment was tweaked by controlling the counterion or changing the dielectric constant of the solvent [10]. Weiss and co-workers have shown that the counterions affect the structure and rheology of short oligomers [9]. Molecular insight attained by Agrawal et al. [16] showed that increasing the dielectric constant of the system decreases the cluster size, affecting their shape, and enhances the dynamics of SPS melt systems. Our quasi-elastic neutron scattering (QENS) studies, have shown that the addition of small amounts of high dielectric solvents such as ethanol to SPS solutions in cyclohexane increases segmental dynamics on short length scales [6]. This enhanced motion has been attributed to reduced cluster dimensions in presence of ethanol, impacting the number of unique chains that reside in each of the clusters, thus reducing the bridging that controls the network. These studies have clearly shown that clustering affects the overall motion of the networks from directly confined network to macroscopic rheology response.

However, the explicit correlation between internal cluster dynamics, across length scales to the mesoscopic and macroscopic motion of ionomer networks, critical to the ability to tune the structure of these complex fluids, remains an outstanding challenge. This fundamental challenge is probed herein, through temperature and dielectric perturbations of the system, while simultaneously following their effects on intra-cluster characteristics and network dynamics.

II-Methodology

A. Systems

Polystyrene sulfonate in its acid form with a molecular weight of ~11 kg/mol with a polydispersity index of 1.2 was purchased from Polymer Source™ Inc. The polymers were synthesized by anionic polymerization and were randomly sulfonated to sulfonation fractions of f = 0.03 of the available sites. NSE samples were made by dissolving 10 wt % of the polymer in *d*-toluene and a 95:5 *d*-toluene/d-ethanol (Tol/EtOH) mixture purchased from Cambridge Isotope Laboratories, Inc., USA. At these low concentrations, the polymer readily dissolves. Samples were then allowed to equilibrate for several days under ambient conditions. The polymer concentration is typical of that used in solution casting of ionic polymers and above the overlap concentration (~6.4 wt %) of the polystyrene with similar molecular weights. Computationally, in addition to the 95:5 Tol/EtOH mixture studied by NSE, we also studied SPS in a 75:25 Tol/EtOH solution. The computational system size for all samples has been chosen to match the largest length scale probed by the NSE.

B. Neutron Spin Echo

The neutron spin echo experiments were performed at the spallation neutron source (SNS) [17], combining data from wavelengths 8 Å and 11 Å and Fourier times of 0.04 –100 ns. A sheet of graphite, and Al_2O_3 powder, were measured and used to correct for instrument resolution. The solvents were run separately and subtracted from the data. The data were collected by an in-house program, and reduced to the form of $S(q,t)$ using the DrSpine program [18]. The temperature was controlled by SP FTS ThermoJet system with the accuracy of +/-0.5 K.

Samples were encapsulated in 3 mm thick quartz rectangular Hellma cells (Müllheim, Germany). Temperature dependence runs were carried out over a smaller q to enable measurements of all temperatures on the same solution. $S(q,t)$ were analyzed as a sum of two exponentials, extracting

relaxation rates for a slow and a fast processes [19]. Results are reported with χ^2 values between of 4-6, depending on the specific solution, with an overall 10% error for the individual fitting parameters. Because of the heterogeneity of the networks, the NSE studies presented herein required intensive resources. To attain a signal to noise ratio sufficient for a reliable analysis, and availability of NSE time, results in an exceedingly long time to accumulate the data.

C. Molecular Dynamics Simulations

Sulfonated polystyrene, toluene and ethanol were built using the polymer builder in BIOVIA™ Materials Studio. The system contained 148 unique, atatic sulfonated polystyrene chains with sulfonation fraction f = 0, 0.03 and 0.09, each with a total molecular weight of ~11 kg/mol with 106 monomer per chain with Na^+ as a counterion. As in the experiments, the computer solutions consist of 10 wt % polymer in pure toluene and toluene, ethanol mixtures. Each system contains between 2.4 - 2.5 million atoms. These large system sizes were used to show that the simulations contained a representative number of chains and to be able to access the range of wave vectors q studied in the NSE experiments.

The all atoms optimized potentials for liquid simulations (OPLS-AA) force fields, developed by Jorgensen et al. [20,21] were used to model the system. This potential includes bonded and non-bonded terms. The bonded potential is sum of intermolecular bond, angle, and dihedral interactions. The non-bonded interactions are described by Lennard-Jones potential with an attractive r^{-6} and repulsive r^{-12} terms and a long-range Coulomb interaction.

Simulations were initially carried out using LAMMPS [22]. The Newton equations of motions were integrated using a velocity-Verlet algorithm with a time step of *1 fs*. The Lennard-Jones interactions are truncated at 1.2 nm. The Coulomb interactions are treated with long-range

particle-particle particle-mesh (PPPM) algorithm with a real space cutoff of 1.2 nm and a precision of $5x10^{-4}$. Periodic boundary conditions were used for all simulations.

The solvents were added after the polymer system was run for 100 ns at 300K in an implicit good solvent. Each system was first run at constant pressure of 1 atm using the Nosé-Hoover thermostat and barostat [23,24] for 10 ns to obtain the correct density. The final dimension of the cell is $L \sim 31.0$ nm for the 3 values of f, which is much larger than the size of a polymer chain whose radius of gyration R_g is 28 – 31 Å. To allow the chains to locally equilibrate the dielectric constant, ε, was increased from 1 to 30 to reduce the residual electrostatic screening between ionic groups. The solution systems were run for 30 ns at constant volume after which the dielectric constant was reset to 1.

The LAMMPS data were then converted to GROMACS [25-27] to enhanced efficiency. The electrostatics were treated using particle mesh Ewald [28] (PME) algorithm and Fourier grid spacing of 0.12 nm. All harmonic bonds involving hydrogen atoms were replaced with constraints. The temperature was maintained using the Bussi-Parrinello thermostat (V-rescale) [29] with a time constant of 0.1 ps. The simulations were carried out using 2 fs time step. Each system was then run at a constant volume at T = 300 K for 600-800 ns, which is limited by accessible computational resources for such large systems. Time t = 0 corresponds to the beginning of the run in GROMACS. The evolution of ionic clusters with time is given in Fig. 1, where we see that after a few hundred nanoseconds the average cluster size has plateaued. The temperature was then increased to 328 K and ran at constant pressure for 10 ns and then ran at constant volume for 300-400 ns. These systems represent realistic states of the polymer in solutions that may often be in long lasting kinetically trapped states.

The dynamic structure factor $S(q,t)$ was calculated for the simulated solutions using

$$S(q,t) = \sum_{i,j=1}^{N} b_i\, b_j e^{iq\cdot(r_i(t)-r_j(t))} \;/\; \sum_{i=1}^{N} b_i^2 \qquad (1)$$

where b_i are the neutron scattering lengths[30] of atom i and $\boldsymbol{r}_i(t)$ position of atom i at time t. Due to the periodic boundary conditions, the wavevectors q are limited to $\boldsymbol{q} = 2\pi/L\ (n_x, n_y, n_z)$, where L is the length of the simulation cell and n_x, n_y, and n_z are integers. Since the lowest q values are limited by the size of the simulation cell, the number of molecules has been chosen to fill a simulation box large enough to sample enough q vectors to capture the NSE experiment.

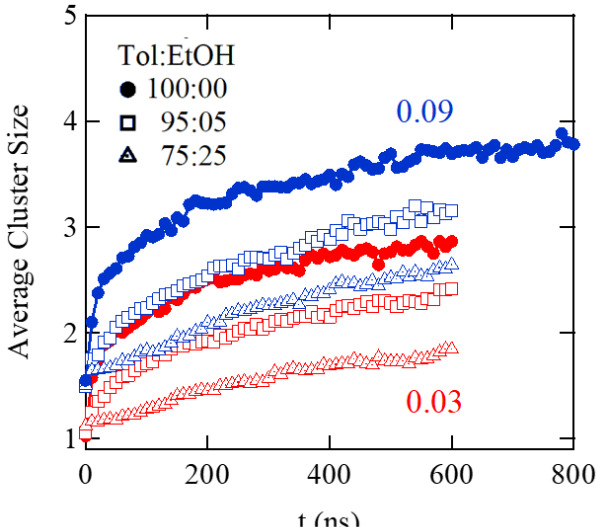

Fig. 1. Cluster size as a function of time for the indicated solutions for f = 0.03 (red) and 0.09 (blue). Cluster size is calculated by the number of S atoms within 6 Å.

III- Results

SPS in tolune solutions form inhomogenous networks driven by long lived ionic assemblies.

These structures have been probbed by SANS [31], revealing a broad signature that captures the correlations of the ionic assemblies, often termed the ionic peak, superimposed on a solution of Guaasian chains. In highly hydrophobic solvents such as tolune, a distinctive signature is observed at very low q valuse corresponding to 500-600 Å and is atributed to large scale instantanous networks. This signature fades with the addition of ethanol, where ethanol decreases the ionic cluster size in these networks. Here NSE measureemnts have been carried out from 0.054 to 0.270 $Å^{-1}$. This range captures the signature that arises from interculster correlations and that of the solvated chains. The very low q range where an instananouse network is observed is not accesable to NSE measurements.

The experimentally measured *S(q,t)* for f=0.03 as ethanol with a dielectric constant ε = 25 is added to toluene whose ε = 2.37 [32,33] are shown in Fig. 2 and are compared with *S(q,t)* measured for toluene [7]. This representation of *S(q,t)* as a function of *t* clearly shows that the overall decay is a result of multiple processes that characterize these clustered complex fluids. The fast dynamics is better observed in a presentation of *S(q,t)* as a function of log *t*, as shown in

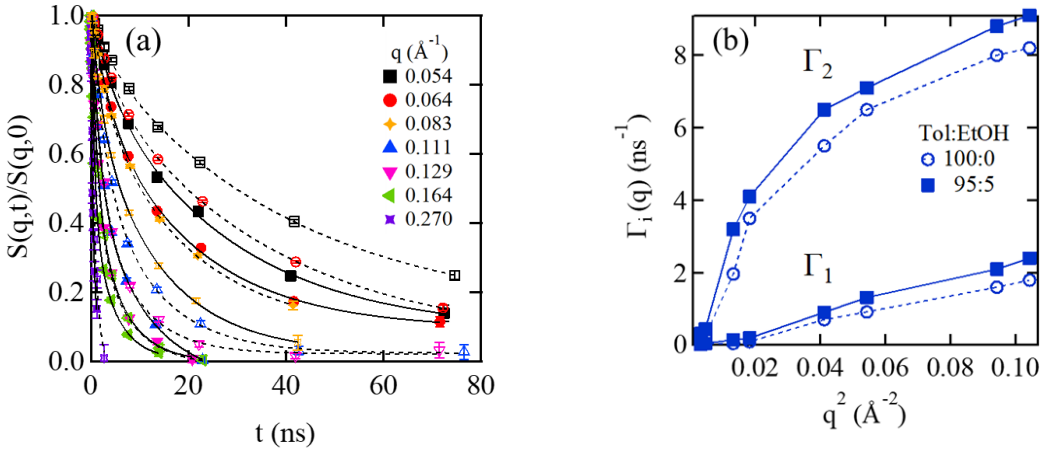

Figure 2: (a) NSE *S(q,t)* for 10 wt % SPS solutions with f = 0.03 at 303 K as a function of time for the indicated q value for 95:5 Tol:EtOH (full lines) in comparison with toluene only (dashed lines) and (b) the relaxation rate constants $\Gamma_1(q)$ and $\Gamma_2(q)$ extracted from the fits to the sum of 2 exponentials for NSE for 95:5 (filled squares) and 100:0 (open circles) Tol:EtOH.

Fig. S1 [34], which highlights the contributions of the fast processes.

As little as 5 wt % ethanol added to toluene is manifested in a significantly faster decay of *S(q,t).* The acceleration of dynamics takes place across all *q* values, with the largest effect is predominantly at the lower *q* regime where the inter ionic clusters correlations are expressed. At higher *q*, where segmental dynamics manifested, *S(q,t)* decays to 0 within 4 – 40 ns and is only slightly affected by the addition of ethanol. This *q* dependence provides direct evidence that cluster characteristics are critical to understanding their impact on mesoscopic motion of the network, where in addition to cluster size and morphology [16,31], inter-cluster dynamic events are critical.

S(q,t) was analyzed in terms of a sum of two exponentials,

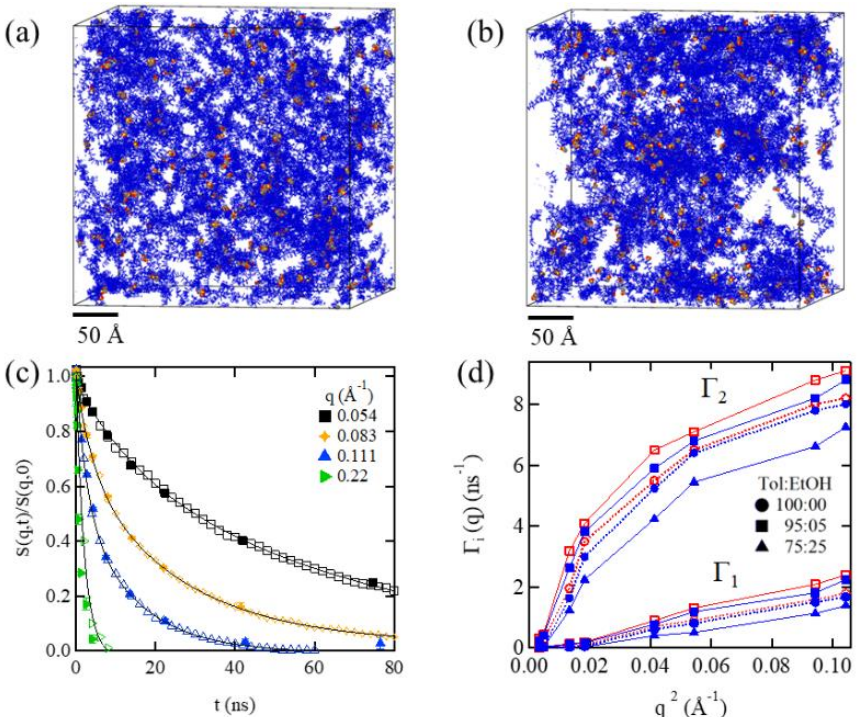

Figure 3: Visualization of 10 wt % *f* = 0.03 SPS in solution of Tol:EtOH (a) 95:5 and (b) 100:0, at 600 ns (blue−polymer backbone, red−oxygen, yellow−sulfur, black-Na) Solvent molecules are removed for clarity. (c) comparison of the dynamic structure factor *S(q,t)* as a function of *q* from the simulations (open) and NSE (solid) for Tol:EtOH 95:5. The lines correspond to fitting of the simulation data. (d) Relaxation rate $\Gamma_i(q)$ as a function of q^2, NSE (red) and simulations (blue) for Tol: EtOH 100:00 (circle) 95:5 (square) and 75:25 (triangle) at 300K.

$$S(q,t)/S(q,0) = A_1 exp(-t/\tau_1(q)) + A_2 exp(-t/\tau_2(q)) \qquad (2)$$

where A_1 and A_2 are pre-exponentials that weigh the contributions of each of the process to $S(q,t)$, t is the time, and $\tau_1(q)$ and $\tau_2(q)$ are generelized relaxation times [19,35]. The data were initially fit to a KWW model [36], which was unsuccessful capturing the entire q range for most systems. The data are further discussed as relaxation rates $\Gamma_i(q) = 1/\tau_i(q)$, that for diffusive systems capture the effective diffusion constants. These are plotted as a function of q^2 in Fig. 2b, with $\Gamma_1(q) < \Gamma_2(q)$. The coresponding representation of these data in terms of effective diffusion constants $\Gamma_i(q)/q^2$ are plotted in Fig. S2 [34]. As seen from Figs. 2b and S2, the relaxation rates $\Gamma_i(q)$ do not follow a simple diffusive procceess, as $\Gamma_i(q)/q^2$ is not independent of q. The pre-exponential factors are presented in Table S1 of the SI where $A_1 + A_2 \sim 1$.

The relaxation rates exhibit two distinctive regions, with a crossover at $q^2 \sim 0.02$ Å^{-2}. At low q, the correlations of the inter-cluster dimensions are reflected, and segmental dynamics is expressed predominantly at higher q values. Even though $\Gamma_1(q)$ and $\Gamma_2(q)$ increase across the entire q range as ethanol is added, the dynamics remains that of a confined system.

Visualizations of computed solutions of Tol:EtOH 95:5 and 75:25 are shown in Fig 3a,b. In both solutions, the size of the ionic clusters visually decreases, as shown in the cluster size evolution with time shown in Fig. 1. With increasing ethanol levels, the chains agglomerate enhancing the heterogeneity of the networks for both solutions. However, the effect is more pronounced in the 75:25 Tol:EtOH solution.

S(q,t)/S(q,0) calculated for the computed solutions is in outstanding agreement (with no adjustable parameters) with the experimental measured values, as shown in Fig. 3c. $\Gamma_1(q)$ and $\Gamma_2(q)$ extracted from fitting *S(q,t)* for the computed solutions and for NSE measurements are presented in Fig. 3d. $\Gamma_1(q)$ and $\Gamma_2(q)$ for 95:5 Tol:EtOH, are accelerated compared with those of toluene solutions, whereas for 75:25 Tol:EtOH are slower. The *q* dependence for both solutions follow that of toluene swollen networks.

The networks are perturbed by increasing the temperature in the NSE experiment from 283K to 328 K for *f=0.03* in toluene and 95:5 toluene-ethanol. Representative NSE spectra for low, intermediate, and high *q* regions for different temperatures are shown in Fig. 4 and the corresponding $\Gamma_1(q)$ and Γ_2(q) are presented in Fig. 5. The temperature range chosen reflects the

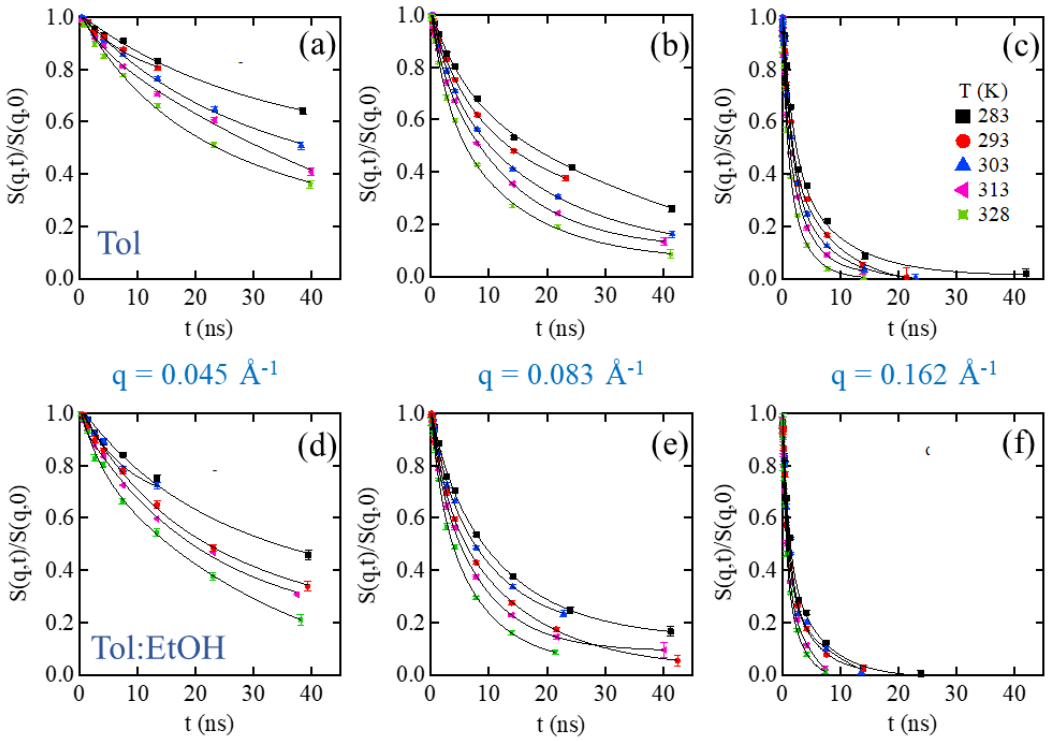

Figure 4: Representative NSE dynamic structure factor *S(q,t)* for 10 wt % solutions of SPS *f* = 0.03 in toluene at *q* = 0.045 Å^{-1}, 0.083 Å^{-1} and 0.165 Å^{-1} and for *f* = 0.03 in 100:0 (top row) and 95:5 (bottom row) Tol:EtOH at the indicated temperatures. The solid lines are the fits to the sum of two exponentials, eq. 2.

fact that in melts, the glass transition temperature of the ionic clusters is on the order of ~ 480 - 550K, depending on the polymer. The lifetime of the ionic clusters in these systems are governed by electrostatic forces [37], which have energies on the order of 10-20 k_BT. There are no direct measurements of the temperature that is necessary to affect the cohesion of the ionic clusters in the systems under consideration. This temperature, however, is above the temperature where the solvents remain liquid in ambient pressures. Thus, we chose an experimentally accessible temperature range and followed the response of the chains.

The results for *S(q,t)* plotted as a function of log *t* are plotted in Fig. S3 [34], which enables easier visualization of the fast processes. With increasing temperature *S(q,t)* decays faster for both solutions, as expected. However, the response of the Tol:EtOH solutions to temperature

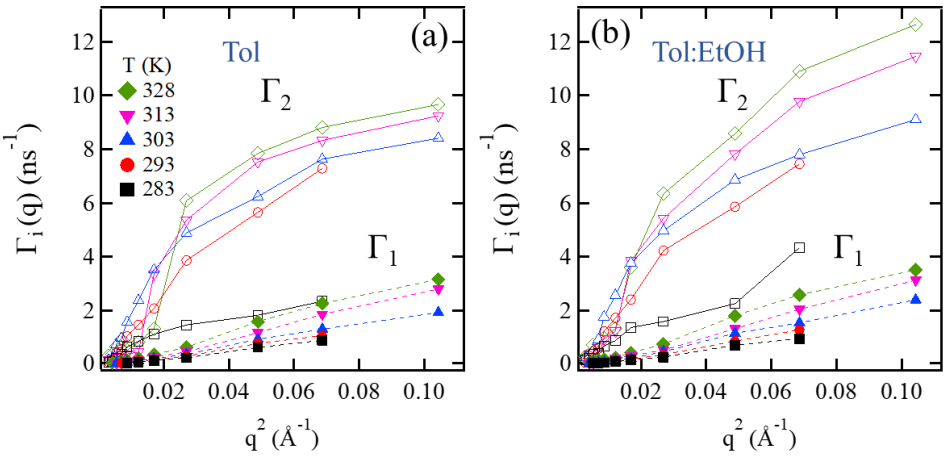

Figure 5: Relaxation rates $\Gamma_1(q)$ (dashed lines) and $\Gamma_2(q)$ (solid lines) a function of q^2 for 10% SPS solutions for the NSE spectra in (a) toluene and (b) 95:5 Tol:EtOH, at the indicated temperatures for f = 0.03.

increase is larger than that of toluene solutions. Part, but not all, of the decrease in relaxation rates with increasing temperature is due to the decrease in viscosity of the solvent. For toluene, increasing the temperature from 283 to 328 K reduces the viscosity by a factor of 1.6 [38]. For the same temperature range, the slowest relaxation rate $\Gamma_1(q)$ increases by a factor of 2.6, independent of q, while the fastest rate increases with a non-monotonic dependence on q and varies from 1 to 5.

At all temperatures, $\Gamma_1(q)$ and $\Gamma_2(q)$ exhibit two distinct length scales with a cross over region. However, at low q, $\Gamma_1(q)$ hardly changes up to $q \sim 0.1$ Å^{-1}, and above, it increases almost linearly. $\Gamma_2(q)$, the faster motion constant, exhibits a similar trend however the crossover takes place across a broader q range. In this temperature range, despite the enhanced motion, the dependence $\Gamma_i(q)$ on q^2 diverge from linearity as the chains remain confined.

$\Gamma_i(q)$ are plotted as a function of *1/T* for selected q values in Figure 6. At low q, increasing temperature has a minimal effect on $\Gamma_1(q)$. However, at higher q, $\Gamma_1(q)$ varies significantly more with temperature. $\Gamma_2(q)$ increases with increasing temperature for all q values. Both $\Gamma_i(q)$ increase with increasing temperature, where the slow relaxation constant, is linear within the accuracy of the fitting which is ~ 10%. The faster relaxation rate diverges from linearity with a crossover at

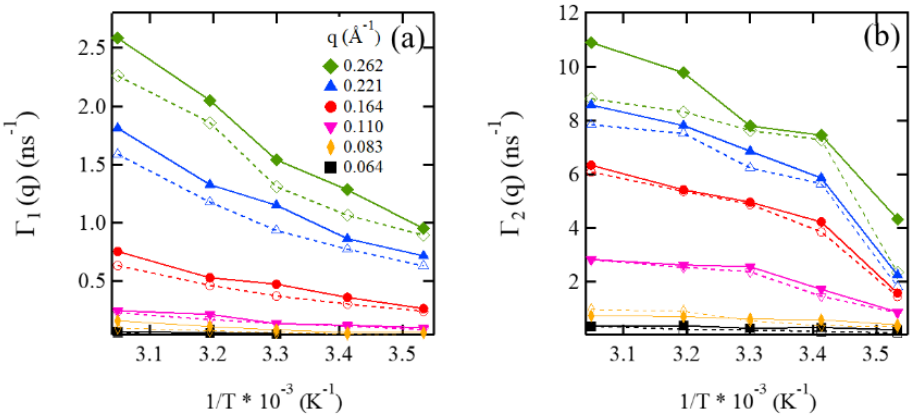

Figure 6. Relaxation rates (a) $\Gamma_1(q)$ and (b) $\Gamma_2(q)$ for the NSE spectra as a function of 1/T for f = 0.03 in 10 wt % SPS toluene (open) and 95:5 Tol:EtOH (filled) solutions at the indicated q values.

~303K. The difference in temperature response reveals that cluster intercorrelation is hardly affected by temperature. The temperature, however, affects segmental motion of the highly solvated chains. Elevating the temperature from 283 to 328 K results in a small energy change of ~ 0.09 kcal/mol, which is significantly smaller than the electrostatic energy that holds together ionizable clusters however it is sufficient to impact solvated segmental dynamics.

This trend however is more pronouced in Tol:EtOH solutions where the clusters are perturbed. Together with previous observations of the impact of added alcohol on the structure [31] ionizable polymers, it is evident that the internal dynamics of the clusters alters the overall motion of the polyemrs on the mesoscopic length scale.

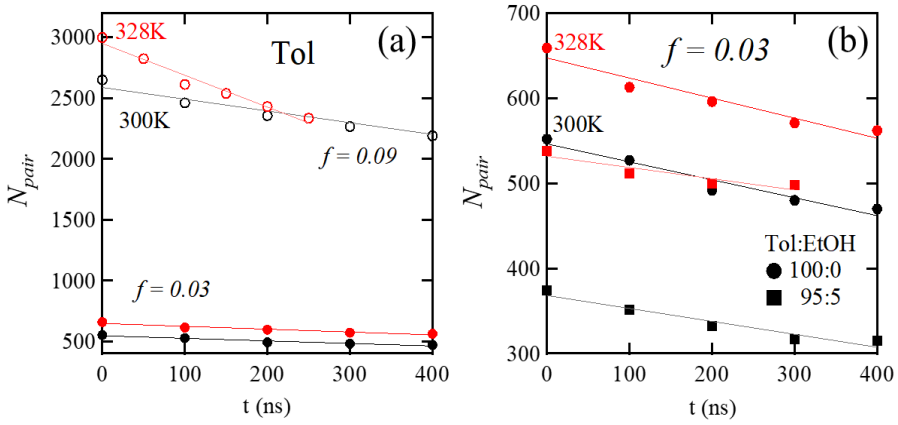

Figure 7: The number of S-S pairs at $t = 0$ that reside in a distinctive cluster and remain in that cluster as a function of time in 10 wt % SPS a) in toluene for $f = 0.03$ (filled) and $f = 0.09$ (open) b) in toluene (circles) and Tol:EtOH (squares) for $f = 0.03$ at 300K (black) and 328K (red).

The internal dynamics of the clusters including the survivial time of pairs of sulfonated groups across the solutions and the time dependance of the intra-cluster correlations were calculated for the simulated solusions. The survival time of pairs of sulfur atoms that initally reside in the same ionic clusters as time evolves, are shown in Fig. 8a for *f=0.03* and *f=0.09* in toluene at two temperatures. Surprisingly, though over long times their number decreases; there is hardly any exchange of ionizable groups between clusters over the time of the network dynamcis. Though the addition of alcohol changes the total number of pairs, seen in Fig. 8b, the average cluster size increases (Fig. 1), the rate at which sulfur atoms leave the clusters remain the same, independend of the presence of alcohol.

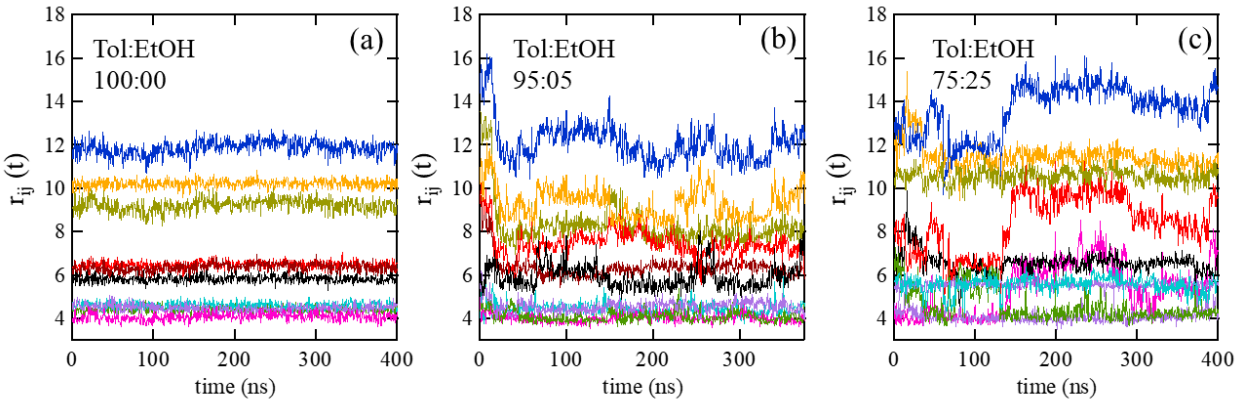

Figure 8: Distance $r_{ij}(t)$ between all sulfur atoms i and j in a representative cluster of size 6 as a function of time for 10 wt % SPS with $f = 0.09$ for Tol:EtOH a) 100:0 b) 95:5 and c) 75:5.

The internal dynamics of the cluster was followed through measurement of the distance $r_{ij}(t)$ between all sulfur atoms *i* and *j* that reside in an ionic cluster, as a function of time. Shown in Fig. 8 are the results for all 15 S-S pairs for a representative cluster of size 6 for f = 0.09 with Tol:EtOH ratios of 100:0, 95:5 and 75:25. In pure toluene, the cluster moves as a rigid body with no exchange of neighbors and little fluctuations in the internal distances over 400 ns. Raising the temperature to 328K, does not affect this pattern. With the addition of ethanol, the sulfur atoms within the cluster become more dynamic where $r_{ij}(t)$ increases over the 400 ns. At the higher temperature, intra cluster neighbor exchanges, which is strongly manifested in 75:25 Tol:EtOH.

Screening the electrostatic interactions by ethanol, even though the solvent molecules remain localized around the cluster, is sufficient to allow internal motion that enables the clusters to morph and change their shape. As it has been previously shown, the shape of the clusters affects network dynamics on the length scale captured by NSE [16]. Therefore, this dynamics on short time scales, is coupled through instantaneous shape change to the much slower motion of the clusters and the entire network.

IV-Conclusions

With insight from NSE measurements and real space results, from MD simulations, we were able to extract and bridge dynamic events across the time and length scales that control the behavior of highly heterogeneous networks formed by solutions of ionizable polymers. A unique agreement between *S(q,t)* extracted from both techniques allows transposing of data across length scales from intra cluster events to that of the networks. *S(q,t)* is analyzed in terms of two characteristic relaxation rates, slow and fast, where the slow one is associated with inter ionic

cluster correlations and the faster one captures segmental dynamics of the solvated chains. Internal cluster dynamics is attained from MD simulations.

In both networks, the clusters are long lived, and significant numbers of sulfur pairs remain in the same clusters for 600-800ns, with very little exchange of ionizable groups between the clusters. In toluene, the internal structure of these clusters hardly changes with time and is not affected by temperature, while the network, however, remains dynamic on the mesoscopic length scale, as evident by NSE measurements. The addition of a polar solvent hardly affects the survival times of the clusters, but does affect the intrinsic dynamics, allowing the clusters to morph and in turn enhances the network dynamics. Temperature enhances the dynamics of the solvated chains independent of the nature of the solvent.

With this two-prong approach, this study was able to identify the dynamics within ionic clusters of a model highly swollen ionic polymer network and provide a first direct correlation between intrinsic dynamics of the ionic assemblies and that of the network. Beyond the impact of the results on ionic polymers' enabling technologies, this approach of combining neutron scattering and simulation would impact a broad range of soft matter systems that are governed by highly distinctive interactions.

ACKNOWLEDGEMENTS

DP gratefully acknowledges DOE grant DE-SC0019284 for support. NSE measurements were carried at ORNL's spallation neutron source. The authors kindly acknowledge the use of computational resources provided by NSF MRI-1725573. This work was made possible in part by advanced computational resources deployed and maintained by Clemson Computing and Information Technology. This research used resources at the National Energy Research

Scientific Computing Center (NERSC), a U.S. Department of Energy Office of Science User Facility operated under contract no. DE-AC02-05CH11231. This work was performed, in part, at the Center for Integrated Nanotechnologies, an Office of Science User Facility operated for the U.S. Department of Energy (DOE) Office of Science. Sandia National Laboratories is a multi-mission laboratory managed and operated by National Technology & Engineering Solutions of Sandia, LLC, a wholly owned subsidiary of Honeywell International, Inc., for the U.S. DOEs National Nuclear Security Administration under contract no. DE-NA-0003525. The views expressed in this article do not necessarily represent the views of the U.S. DOE or the United States Government

*Corresponding authors: C. Kosgallana (ckosgal@g.clemson.edu); G. S. Grest (gsgrest@sandia.gov); D. Perahia (dperahi@g.clemson.edu)

[&]*Current address*: Neutron Scattering Division, Oak Ridge National Laboratory, Oak Ridge, TN 37831, USA

[#]*Current address:* Materials Science Division, Lawrence Livermore National Laboratory, Livermore, CA 94550, USA

References

[1] J. K. Lee *et al.*, *Ionomer-free and recyclable porous-transport electrode for high-performing proton-exchange-membrane water electrolysis*, Nature Communications **14**, 4592 (2023).

[2] P. Balding, R. Borrelli, R. Volkovinsky, and P. S. Russo, *Physical properties of sodium poly (styrene sulfonate): comparison to incompletely sulfonated polystyrene*, Macromolecules **55**, 1747 (2022).

[3] Z. Malik, N. Muhammad, M. Kaleem, M. Nayyar, A. S. Qazi, D. Q. Butt, S. Z. Safi, and A. S. Khan, *Anticariogenic and Mechanical Characteristics of Resin-Modified Glass Ionomer Cement Containing Lignin-Decorated Zinc Oxide Nanoparticles*, ACS Applied Bio Materials **6**, 425 (2023).

[4] S. Favero, I. E. Stephens, and M. M. Titirci, *Anion Exchange Ionomers: Design Considerations and Recent Advances-An Electrochemical Perspective*, Adv. Mat., 2308238 (2023).

[5] L. R. Middleton and K. I. Winey, *Nanoscale aggregation in acid-and ion-containing polymers*, Annual review of chemical and biomolecular engineering **8**, 499 (2017).

[6] S. S. Mohottalalage, C. Kosgallana, M. Senanayake, S. Wijesinghe, N. C. Osti, and D. Perahia, *Molecular Insight into the Effects of Clustering on the Dynamics of Ionomers in Solutions*, ACS Macro Lett. **12**, 1118 (2023).
[7] C. Kosgallana, S. Wijesinghe, M. Senanayake, S. Mohottalalage, M. Ohl, P. Zolnierczuk, G. S. Grest, and D. Perahia, *From Molecular Constraints to Macroscopic Dynamics in Associative Networks formed by Ionizable Polymers: A Neutron Spin Echo and Molecular Dynamics Simulations Study*, ACS Polymers Au (2024).
[8] J. Fitzgerald, D. Kim, and R. Weiss, *The effect of diluents on the ionic interactions in sulfonated polystyrene ionomers*, Journal of Polymer Science Part C: Polymer Letters **24**, 263 (1986).
[9] K. Chakrabarty, T. Seery, and R. Weiss, *Characterization of ionomer solutions. 1. Phase behavior and gelation of sulfonated polystyrene ionomers in decalin*, Macromolecules **31**, 7385 (1998).
[10] R. Weiss and W.-C. Yu, *Viscoelastic behavior of very lightly sulfonated polystyrene ionomers*, Macromolecules **40**, 3640 (2007).
[11] R. Weiss and H. Zhao, *Rheological behavior of oligomeric ionomers*, Journal of Rheology **53**, 191 (2009).
[12] X. Qiao and R. A. Weiss, *Nonlinear Rheology of Lightly Sulfonated Polystyrene Ionomers*, Macromolecules **46**, 2417 (2013).
[13] Q. Chen, C. Huang, R. Weiss, and R. H. Colby, *Viscoelasticity of reversible gelation for ionomers*, Macromolecules **48**, 1221 (2015).
[14] E. De Luca, T. A. Waigh, M. Monkenbusch, J. S. Kim, and H. S. Jeon, *Neutron spin echo study of the dynamics of micellar solutions of randomly sulphonated polystyrene*, Polymer **48**, 3930 (2007).
[15] B. Nyström, J. Roots, J. Higgins, B. Gabrys, D. Peiffer, F. Mezei, and B. Sarkissian, *Dynamics of polystyrene sulfonate ionomers in solution. A neutron spin-echo study*, Journal of Polymer Science Part C: Polymer Letters **24**, 273 (1986).
[16] A. Agrawal, D. Perahia, and G. S. Grest, *Clustering effects in ionic polymers: Molecular dynamics simulations*, Phys. Rev. E **92**, 022601 (2015).
[17] M. Ohl *et al.*, *The spin-echo spectrometer at the Spallation Neutron Source (SNS)*, Nuclear Instruments and Methods in Physics Research Section A: Accelerators, Spectrometers, Detectors and Associated Equipment **696**, 85 (2012).
[18] P. Zolnierczuk, O. Holderer, S. Pasini, T. Kozielewski, L. Stingaciu, and M. Monkenbusch, *Efficient data extraction from neutron time-of-flight spin-echo raw data*, Journal of applied crystallography **52**, 1022 (2019).
[19] D. Richter, M. Monkenbusch, A. Arbe, and J. Colmenero, *Neutron spin echo in polymer systems* (Springer, Berlin, 2005).
[20] W. L. Jorgensen, D. S. Maxwell, and J. Tirado-Rives, *Development and testing of the OPLS all-atom force field on conformational energetics and properties of organic liquids*, Journal of the American Chemical Society **118**, 11225 (1996).
[21] W. L. Jorgensen, J. D. Madura, and C. J. Swenson, *Optimized intermolecular potential functions for liquid hydrocarbons*, Journal of the American Chemical Society **106**, 6638 (1984).
[22] A. P. Thompson *et al.*, *LAMMPS-A flexible simulation tool for particle-based materials modeling at the atomic, meso, and continuum scales*, Comp. Phys. Comm. **271**, 108171 (2022).
[23] S. Nosé, *A unified formulation of the constant temperature molecular dynamics methods*, The Journal of chemical physics **81**, 511 (1984).

[24] W. G. Hoover, *Canonical dynamics: Equilibrium phase-space distributions*, Physical review A **31**, 1695 (1985).
[25] S. Pronk *et al.*, *GROMACS 4.5: a high-throughput and highly parallel open source molecular simulation toolkit*, Bioinformatics **29**, 845 (2013).
[26] M. J. Abraham, T. Murtola, R. Schulz, S. Páll, J. C. Smith, B. Hess, and E. Lindahl, *GROMACS: High performance molecular simulations through multi-level parallelism from laptops to supercomputers*, SoftwareX **1**, 19 (2015).
[27] H. J. Berendsen, D. van der Spoel, and R. van Drunen, *GROMACS: A message-passing parallel molecular dynamics implementation*, Computer physics communications **91**, 43 (1995).
[28] U. Essmann, L. Perera, M. L. Berkowitz, T. Darden, H. Lee, and L. G. Pedersen, *A smooth particle mesh Ewald method*, The Journal of chemical physics **103**, 8577 (1995).
[29] G. Bussi, D. Donadio, and M. Parrinello, *Canonical sampling through velocity rescaling*, The Journal of chemical physics **126**, 014101 (2007).
[30] https://www.ncnr.nist.gov/resources/n-lengths/ (Accessed 2/7/23).
[31] C. Kosgallana, M. Senanayake, S. Wijesinghe, S. Mohottalalage, L. He, G. S. Grest, and D. Perahia, *Clustering Effects on the Structure of Ionomer Solutions: A Combined SANS and Simulations Study*, Macromolecules (2024).
[32] M. Mohsen-Nia, H. Amiri, and B. Jazi, *Dielectric constants of water, methanol, ethanol, butanol and acetone: measurement and computational study*, J. Solution Chem. **39**, 701 (2010).
[33] A. Jezuita, P. A. Wieczorkiewicz, H. Szatylowicz, and T. M. Krygowski, *Effect of the Solvent and Substituent on Tautomeric Preferences of Amine-Adenine Tautomers*, ACS omega **6**, 18890 (2021).
[34] *See Supplemental Material at [URL will be inserted by publisher] for figures that present S(q,t) vs log t, that are paired with the data presented in the body of the paper as S(q,t) vs t. This representation of the data allows a better visualization of the fast processes in the system. It also includes a presentation of the effective diffusion coefficients* $\Gamma_i(q)/q^2$ *extracted from the fitting of the NSE data as a function of q and a table of the pre-exponential fitting parameters* A_1 *and* A_2 *as a function of q for the experimental systems.*
[35] F. Mezei, W. Knaak, and B. Farago, *Neutron spin echo study of dynamic correlations near liquid-glass transition*, Physica Scripta **1987**, 363 (1987).
[36] N. Rabiei, S. H. Amirshahi, and M. H. Kish, *Description of physical aging kinetics of glassy polymers by interpretation of parameters of the Kohlrausch-Williams-Watts relaxation function via simulation*, Physical Review E **99**, 032502 (2019).
[37] B. Dreyfus, *Model for the clustering of multiplets in ionomers*, Macromolecules **18**, 284 (1985).
[38] F. J. Santos, C. A. Nieto de Castro, J. H. Dymond, N. K. Dalaouti, M. J. Assael, and A. Nagashima, *Standard reference data for the viscosity of toluene*, J. Phys. Chem. Ref. Data **35**, 1 (2006).